

Reactions of Gas Phase Monomers with Radicals on the Surface of Silica: Reversibility of the Radical Addition Reaction in the SO₂–Alkene System

Dmitri V. Vezenov,* Vladimir B. Golubev, and Valeri P. Melnikov

N. N. Semenov Institute of Chemical Physics of the Russian Academy of Sciences, Moscow, Russia

Received July 15, 2002; Revised Manuscript Received January 9, 2003

ABSTRACT: Chemically and mechanically activated silica provides a convenient system to prepare surface stabilized radicals of the chosen type. A combination of the volumetric techniques and electron spin resonance spectroscopy was used to characterize the reactions of para- and diamagnetic defects on the surface of the activated silica with simple molecules (H₂, O₂, CO, CO₂, SO₂) and monomers (ethylene, tetrafluoroethylene, cyclopentene, methyl acrylate, and allyl alcohol) from the gas phase. Bimolecular rate constants as high as 10⁶ L·mol⁻¹·s⁻¹ could be determined. A significantly strong adsorption of the molecules containing polar groups was shown to be a limitation for the kinetics experiments with surface-grafted radicals. The study of the kinetics of the cross-reactions in the alternating radical copolymerization of SO₂ with alkenes was carried out in the regime of the “stopped chain growth”. The reversibility of the SO₂ addition to alkyl radicals was observed in *real time* with the stability (at 298 K) of the sulfonyl radicals decreasing in the order ≡SiC₂F₄SO₂· ($K_{eq} > 10^{16}$ L·mol⁻¹) > ≡SiC₂H₄SO₂· ($K_{eq} = 4.9 \times 10^8$ L·mol⁻¹) > ≡SiC₅H₁₀SO₂· ($K_{eq} = 6.8 \times 10^7$ L·mol⁻¹). The rate constants at 298 K for the SO₂ addition were found to be >10⁷, 59 ($\Delta E_a \sim 9.3$ kJ·mol⁻¹), and 1.7×10^4 L·mol⁻¹·s⁻¹ in this sequence. The corresponding rate constants for the SO₂ dissociation were 1.2×10^{-7} and 2.5×10^{-4} s⁻¹ for the ethylsulfonyl and cyclopentylsulfonyl radicals; tetrafluoroethylsulfonyl radicals were stable in the temperature range studied (up to 373 K). An activation energy of ~ 9 kJ·mol⁻¹ for the SO₂ addition to ethyl radicals was determined, while a reverse reaction was characterized by 87.6 kJ·mol⁻¹ activation energy, in agreement with the previous work. Alkenes were found totally unreactive toward sulfonyl radicals at temperatures up to 373 K and pressures up to 1 atm ($K_{eq} < 10^{-6}$ L·mol⁻¹). The implications of these results for the mechanism of the alternating copolymerization are discussed.

Introduction

The characterization of the mechanism and kinetics of radical reactions is challenging due to extreme reactivity of the radical species. Side reactions often compete with the process of the primary interest. The presence of the secondary radicals frequently makes it difficult to discriminate between the individual elemental steps of the overall rapid process of the radical interconversion. Thus, information about the relative reactivity of radicals and monomers is often derived from the composition of the copolymers formed. A short lifetime of radicals makes their spectroscopic characterization difficult and often requires the use of some stopped flow or trapping techniques. An alternative means to avoid numerous reaction pathways is to stabilize the radical reaction centers by grafting them onto an inert solid support. The chemical reaction can then be carried out from the gaseous phase of a controlled composition, while the rates of such reactions can be adjusted by choosing appropriate pressures of the gas-phase reactants.

The surface of silica is an attractive system, with which one can use this approach. The method of obtaining paramagnetic centers of the preassigned structure on the surface of the activated SiO₂ has been developed and used successfully to study the mechanism and kinetics of several radical reactions.^{1–5} The formation of the para- and diamagnetic centers of chemisorption on the surface of the silicon dioxide occurs upon a thermal activation of methoxylated silica^{4,5} (≡Si· and

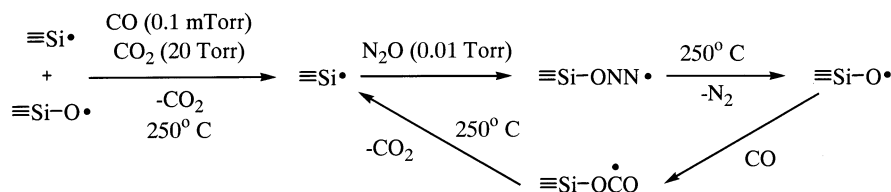
≡Si: centers) or a mechanical activation of silica and also quartz^{1–3} (≡SiO·, ≡Si·, ≡Si: and ≡Si=O centers). The active sites can be quantitatively converted from one form into another by a treatment with the appropriate gases and a specific type of reactive centers can be obtained on the surface¹ (Schemes 1 and 2). Recently, the reactions of adsorption and thermal decomposition of CH₃OH on the surface of SiO₂ were thoroughly characterized using IR spectroscopy⁶ and temperature-programmed desorption.⁷ A formation of the free radical sites upon pyrolysis was asserted.

A radical chain reaction on the surface of SiO₂ can be carried out in the fashion of a “stopped chain growth” by dosing small amounts of a reactant (monomer) from the gaseous phase. A rate constant of an elemental chemical act can then be obtained from the rate of the disappearance of the reactant in the gaseous phase with a simultaneous monitoring of the chemistry of the process by the electron spin resonance (ESR).^{2,5} Radical copolymerization reactions are especially amenable to being studied with this approach, since the degree of conversion can be easily monitored and the monomers can be changed in a stepwise manner to model the two possible cross-reactions.

The present work applies the general approach of creating stable radicals grafted to the SiO₂ surface to examine the reactions of these sites with monomers from the gaseous phase. Our primary interest was in the formation of the sulfonyl radicals and their reactivity toward olefins. The direct observation of the radical intermediates in this reaction can provide insights into the mechanism of the alternating copolymerization of olefins with sulfur dioxide leading to polysulfones.⁸ In

* Corresponding author. Current address: Nanoptek, Inc., P.O. Box 1542, Concord, MA, 01742.

Scheme 1. Chemical Reactions Used to Create Chemically Homogeneous Radicals on the Surface of Mechanically Activated Silica or Quartz (Breaking of Si–O–Si Bonds)



Scheme 2. Reactions Used to Create Chemically Homogeneous Surface Radicals in the Case of Chemically Activated Silica (Breaking of Si–O–C Bonds)

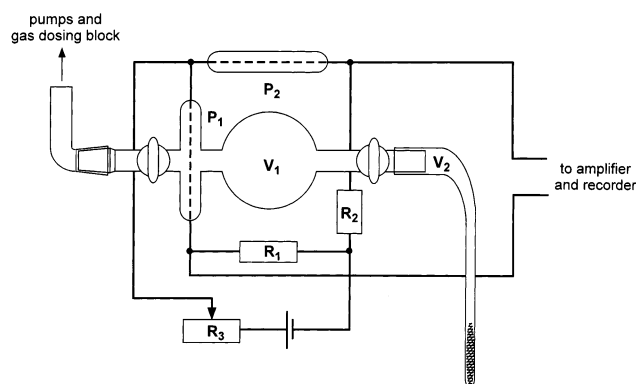
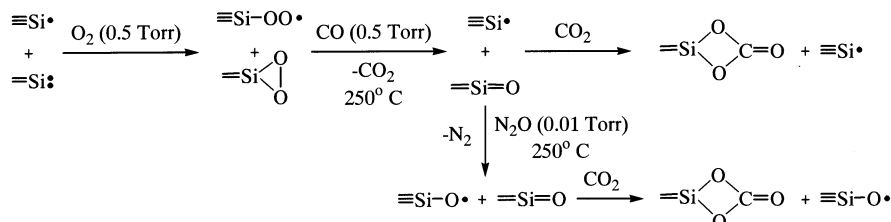


Figure 1. Diagram of the reaction module used in the kinetics experiments. A variable resistor R_3 was used to balance a bridge consisting of two Pirani monometers (P_1 and P_2) and two resistors (R_1 and R_2). Changing gas pressure in P_1 resulted in an unbalanced bridge and was recorded as the reaction progressed in the volume V_2 .

solution, the addition of SO_2 is known to proceed very fast with the rate constants on the order of $10^8 \text{ L}\cdot\text{mol}^{-1}\cdot\text{s}^{-1}$,^{8,9} so that even the traces of peroxides in the olefin– SO_2 mixture can lead to a spontaneous formation of the polysulfones.⁹ We employed the technique of stabilizing radicals on the SiO_2 surface to investigate the kinetics of the radical reactions in the activated silica–monomer and SO_2 –alkene systems.

Experimental Section

Vacuum System. A glass vacuum apparatus was constructed for this work. The experimental setup included the following blocks: (1) diffusion and adsorption vacuum pumps; (2) pressure meters and vacuum gauges; (3) a block for the storage of gases, preparation of gas mixtures and dosage of small portions of gases; (4) a reaction cell. The vacuum system was assembled in the close vicinity of the ESR spectrometer. The reaction cell was connected to the vacuum system by means of a multijoint glass arm, which allowed us to translate the sample (under vacuum) freely in space and insert it into a resonator of the ESR spectrometer to record the spectra (Figure 1). A precise automatic measurement of the low gas pressure was performed by means of the Pirani manometer P_1 with a sensitivity of $(0.7\text{--}2.5) \times 10^{-6} \text{ Torr/mV}$ at a bridge current of 30 mA. The manometer was calibrated in the range of its linear response ($\leq 10^{-2} \text{ Torr}$) for every gas used.

Reaction Cell. A radical reaction on the surface of SiO_2 was carried out by bringing a portion of a gaseous reactant

from the reaction volume V_1 into contact with a sample of activated SiO_2 in the volume V_2 (Figure 1). SiO_2 was poured from the ESR ampule into a wider section of the cell prior to the reaction and shaken at 50 Hz by a mechanical vibrator during the reaction. The pressure drop in the course of the reaction was recorded automatically. After the completion of the reaction, the SiO_2 powder was poured back into the ESR ampule and a spectrum of the formed radical was taken. The reaction cell was designed to operate with portions of gases as small as $(1\text{--}5) \times 10^{15}$ molecules (1–10 nmol), corresponding to approximately 10% of the overall number of the radical centers in the sample.

ESR Spectra. The ESR spectra were taken on an X band (3 cm) ESR spectrometer (Institute of Chemical Physics of the Russian Academy of Sciences) with a high-frequency modulation of 100 kHz. The signals of the paramagnetic centers trapped in the solid matrix and, therefore, not accessible to the molecules from the gaseous phase were used as internal standards. Radicals $\equiv\text{Si}\cdot$ and $\equiv\text{C}\cdot$ served this purpose in the cases of mechanically and chemically activated SiO_2 , respectively. The intensities of all peaks were normalized with respect to these standard signals to account for a slightly different positioning of the ESR ampule every time the sample was reinserted into the resonator. The intensity of the ESR signal was determined as an amplitude of a chosen spectral line. This approach was expected to be sufficient if no line shape changes occurred. Since only the ratios of intensities of the ESR spectra for the same radical were used to derive kinetic results, the approach was found generally valid in our case. We observed a linear relationship between the ESR signal intensity defined in the above manner and the molar amount of a gaseous reagent consumed. The g factors and the hyperfine structure splitting, a , were calibrated with respect to the third and fourth components in the spectrum of Mn^{2+} ions in MgO matrix ($g = 2.0010$, $a = 87.1 \text{ G}$).

Preparation of Mechanically Activated Silica MSI. Quartz was powdered and the fraction of 0.5–1.0 mm was sieved out. Quartz powder, washed with distilled water and dried at 150°C , was placed in a spherical thick-walled quartz vibromill charged with the quartz beads. The content of the mill was heated at 1000°C for 1 h under inert atmosphere (He) or high vacuum ($<10^{-6} \text{ Torr}$). The mill was then cooled to room temperature, filled with He (100–200 Torr) and sealed off from the vacuum apparatus. Quartz was ground by electromechanical vibrator at the amplitude of 10–12 mm and frequency 50–100 Hz for 0.5–1.0 h at room temperature. The samples were annealed at 500°C for 0.5–1.0 h afterward to decrease the influence of the diamagnetic centers on chemisorption. The mill was designed to permit the transfer of the mechanically activated quartz to the reaction cell without exposure to air. A reaction cell received 0.6–0.8 g of activated SiO_2 , which had a specific surface area of 5–15 m^2/g and

contained $(0.5-1.5) \times 10^{17}$ radicals/g. To obtain the paramagnetic centers of one particular kind ($\equiv\text{Si}^\bullet$ or $\equiv\text{SiO}^\bullet$) and to block the diamagnetic sites of chemisorption, the samples were further treated according to the Scheme 1. The number of radicals was determined by the amount of N₂ formed or CO adsorbed (CO₂ formed): both measurements agreed within 5% accuracy. The specific area was determined from the low temperature (77 K) nitrogen adsorption using the BET equation.

Preparation of Chemically Activated Silica RSi. Various conditions (see Supporting Information) were tried to optimize the thermal activation process of methoxylated aerosil. The standardized procedure was as follows. Aerosil (1–2 g) was placed in the quartz tube, pumped down to 10^{-5} Torr, dried at 500 °C for 0.5 h, and annealed in the oxygen atmosphere (200 Torr) at 900 °C for 0.5 h to remove organic contaminants from its surface. Methoxylation was performed in the atmosphere of methanol vapor (60–100 Torr) by the gradual increase of the temperature from 20 to 400–450 °C at the rate of 10°/min. Methanol was removed by evacuation and the sample was activated under high vacuum (10^{-6} Torr) at 950 °C for 30 min. This time was sufficient for the completion of the pyrolysis process (it was considered complete if the decomposition products that could not be condensed at 77 K, i.e., H₂ and CO, were no longer formed). The rate of the temperature elevation was minimal (5°/min) in the range of 650–750 °C when pyrolysis occurred most vigorously. A reaction cell contained 0.2–0.3 g of activated SiO₂, which had specific area of 75 m²/g and $(4-6) \times 10^{18}$ radicals and $(5-6) \times 10^{19}$ diamagnetic centers per gram. The samples were treated further according to the Scheme 2. All samples had an impurity of $\equiv\text{SiCH}_2^\bullet$, which constituted less than 0.1% of the overall number of radicals in the sample and did not affect the reactions studied in the present work. An attempt to activate ground quartz treated prior to methoxylation by alkaline or acidic solution and washed with distilled water was unsuccessful. No paramagnetic centers were observed in this case.

Kinetic Data Recording in Volumetric Measurements.

The Pirani manometer P₁ measures the pressure in part V₁ of the reaction cell while the chemical reaction takes place in the other part, V₂, of the cell (Figure 1). These parts are separated by a vacuum stopcock and a connecting tube with a membrane, which all constitute a resistance to the gas flow from the volume V₁ to V₂. To observe the actual chemical process, it is necessary that (1) the equilibrium between the pressure P₁ in the volume V₁ and P₂ in V₂ is reached much faster than the consumption of the gas in a chemical reaction and (2) the inertia of the response in the registering system (Pirani manometer, electric circuits, an amplifier, a recorder, etc.) does not impose a significant delay. The evaluation of the dynamic characteristics of the experimental setup resulted in the relaxation time constant $\tau_{\text{setup}}=0.8$ s for our measuring system. The rate constant of the gas flow χ did not depend on the gas pressure by virtue of the molecular regime of the gas flow in the pressure range of our experiments ($\leq 10^{-3}$ Torr):

$$\ln \chi = 1.42 - 0.5 \ln M \quad (4)$$

where M is a molecular weight (in atomic units). Thus, for all gases used in the present study ($M \geq 28$) kinetic curves of the pressure drop are not limited by the sluggishness of the detecting system, since $\tau_{\text{setup}} < \tau_{\text{flow}} = \ln 2/\chi = 0.9$ s.

If the concentration of a reactant in the gaseous phase is assumed to be its acting concentration, then the change of the pressure during the course of the reaction in different parts of the reaction cell can be described by the system of two coupled differential equations:

$$\frac{dP_1}{dt} = -\chi(P_1 - P_2), \quad P_1(0) = P_0 \quad (2)$$

$$\frac{dP_2}{dt} = \chi(P_1 - P_2)\frac{V_1}{V_2} - kNP_2, \quad P_2(0) = 0 \quad (3)$$

where k is the rate constant (in mol⁻¹·s⁻¹) of the radical reaction and N is the number of radicals. Introducing $\mu = (V_1 + V_2)/V_2$, it can be shown that after an initial time period $t > 2/\mu\chi = 0.3-0.7$ s (for our experimental setup, $\chi = 0.3-0.8$ s⁻¹ and $\mu > 10$)

$$P_2(t) = P_1(t)\frac{\mu\chi}{\mu\chi + kN} \quad (4)$$

and the normalized reaction rate $\omega = -(dP/dt)(1/P)$ obeys a law of the summation of "kinetic resistances":

$$\frac{1}{\omega} = \frac{1}{\chi} + \frac{\mu}{kN} \quad (5)$$

If a chemical reaction is relatively slow, that is $\chi \gg kN/\mu$, then $P_2(t) \approx P_1(t)$, and the rate of the pressure drop observed is determined by the kinetics of the chemical reaction on the surface of silica. Under large $k \gg \mu\chi/N$, when a fast chemical process takes place, it follows that $P_2(t) \approx 0$. This latter case corresponds to a physical model of the gas expansion into infinitely large volume, because the state of the "vacuum" is maintained by a fast chemical reaction at the interface. Thus, the upper limit for the determination of k in this reaction module is on the order of 10^8 L·mol⁻¹·s⁻¹.

For comparison to available data on homogeneous reactions, it is more convenient to express the rate of the reaction in terms of the number of surface radicals, N , and molar concentration of the monomer M

$$-\frac{dN(t)}{dt} = k'N(t)[M] \quad (6)$$

where k' is in L·mol⁻¹·s⁻¹. In this form, the description of kinetics in our heterogeneous system becomes entirely equivalent to that of a homogeneous system where instead of the concentration of one of the reactants the total molar amount of this reactant is considered. Realizing that $[M] = P/RT$ and $dN/dt = d(PV/RT)/dt$, we see from comparison with the eq 3 that $k = k'/V$. In what follows, we omit the prime and report the results in the form directly comparable to the rate constants of the homogeneous reactions.

For most of the reactions we investigated, the radicals formed in the reaction with the gas molecules were inert or orders of magnitude less reactive toward this gaseous reactant than the initial paramagnetic centers ($\equiv\text{Si}^\bullet$ and $\equiv\text{SiO}^\bullet$). In these cases, the kinetics observed corresponds to a single chemical reaction and its analysis can be conducted in the following manner. Let N_0 be the number of the initial radicals in the sample, then their amount will be $N_0 - n$ at time t , where n is the number of the initial radicals converted into inactive form. Since n for a bimolecular reaction is equal to the number of the gas molecules that have reacted by the time t , n can be calculated from the pressure vs time curves. Assuming proportionality of the reaction rate to the concentration of the reagent in the gaseous phase and the equivalence of the paramagnetic centers on the solid support throughout the course of the reaction, the bimolecular kinetics in the reaction volume $V = V_1 + V_2$ will be expressed by

$$-\frac{dP(t)}{dt} = \frac{k}{V}P(t)\left(N_0 - \frac{(P_0 - P(t))V}{RT}\right) \quad (7)$$

or, equivalently, by an equation for the normalized rate

$$\omega = \frac{k}{V}(N_0 - n) \quad (8)$$

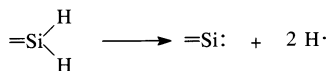
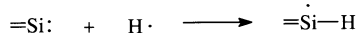
where $\omega = -(dP/dt)(1/P)$ and $n = ((P_0 - P(t))V)/RT$.

Thus, an experimentally observed linear dependence of the normalized reaction rate ω on n will validate the assumption of the proportionality of the reaction rate to the reactant pressure.

Results and Discussion

Reactions of the Defects on the Surface of Silica with H₂, O₂, CO, and CO₂ from the Gaseous Phase.

The procedure for thermal activation of methoxylated silica was originally reported in references.^{10,11} These and a later study⁶ established formation of Si–H bond during pyrolysis based on the IR measurements. The removal of methoxy groups from the surface of methoxylated silica was also investigated by means of the temperature-programmed desorption with mass spectroscopic analysis of the decomposition products.⁷ The reaction of the Si–H bond formation was found to proceed through formaldehyde (CH₂O) evolution, which in turn can produce a mixture of CO and H₂ in certain temperature regimes. The formation of the electron-deficient species (para- and diamagnetic defects) on the surface of silica then occurs via homolytic rupture of Si–H bond at the later stages of pyrolysis. With our experimental setup, we were able to quench $\equiv\text{Si}^\bullet$ radicals with molecular hydrogen and then regenerate them by the second thermal activation step:



Upon treatment with hydrogen, the ESR spectrum of $\equiv\text{Si}^\bullet$ centers transforms into a spectrum of $\equiv\text{Si-H}^\bullet$ paramagnetic centers ($g_\perp = 2.0021$, $g_\parallel = 2.0033$, $a = 80.4$ G) reflecting a general property of the silylene sites to act as radical traps.¹ The latter spectrum disappeared again with a concomitant restoration of the ESR signal of the $\equiv\text{Si}^\bullet$ radicals when the sample was subjected to pyrolysis at 960 °C once again. However, when a similar scheme for molecular oxygen was followed, it was a weak O–O bond in $\equiv\text{Si-O-O}^\bullet$ that was broken upon pyrolysis to form $\equiv\text{SiO}^\bullet$ radicals, easily identified by their reaction with CO.¹

The kinetic approach described in the Experimental Section was applied to the reactions of the paramagnetic and diamagnetic centers with O₂, CO, and CO₂ that were previously known to occur on the surfaces of RSi or MSi (Table 1). Figure 2 typifies the data used in the determination of the rate constants from eq 8 for the reactions compiled in Table 1. The total number of the surface reactive centers can be determined by the extrapolation to zero rate. A quantitative conversion of the reactive centers upon treatment with various simple molecules was found. The observed linear dependence of the normalized reaction rate on the amount of gas molecules dosed confirms the validity of the assumptions made in the derivation of the rate law (eq 8).

A remarkably different reactivity of silyl radicals and silylene centers was observed in their reaction with O₂. This reaction can be used to successfully discriminate between para- and diamagnetic defects of RSi by an abrupt change of the slope in the pressure–time curve for the oxygen chemisorption. The number of the reaction sites found from the chemisorption of O₂ or CO agreed well with the amount of CO₂ formed in the thermal decomposition of the carbonate. However, the subsequent reaction of the siloxane centers with CO₂ revealed their thermal instability. According to a 3-fold decrease in the amount of CO₂ consumed in the second

Table 1. Reactions of the Para- and Diamagnetic Defects on the Surface of Silica with Some Simple Molecules from the Gaseous Phase

Reaction	$N_0 \times 10^{19} \text{ g}^{-1}$	$k, \text{L} \cdot \text{mol}^{-1} \cdot \text{s}^{-1}$
$\equiv\text{Si}^\bullet + \text{O}_2 \xrightarrow{25^\circ\text{C}} \equiv\text{Si-O-O}^\bullet$	0.4	$1.5 \cdot 10^6$
$\equiv\text{Si:} + \text{O}_2 \xrightarrow{25^\circ\text{C}} \equiv\text{Si} \begin{array}{c} \diagup \text{O} \diagdown \\ \diagdown \text{O} \diagup \end{array}$	4.2	$5.0 \cdot 10^2$
$\equiv\text{Si} \begin{array}{c} \diagup \text{O} \diagdown \\ \diagdown \text{O} \diagup \end{array} + \text{CO} \xrightarrow{25^\circ\text{C}} \equiv\text{Si} \begin{array}{c} \diagup \text{O} \diagdown \\ \diagdown \text{O} \diagup \end{array} \text{C=O}$	4.3	$3.0 \cdot 10^3$
$\equiv\text{Si} \begin{array}{c} \diagup \text{O} \diagdown \\ \diagdown \text{O} \diagup \end{array} \text{C=O} \xrightarrow{250^\circ\text{C}} \equiv\text{Si=O} + \text{CO}_2$	4.3	-
$\equiv\text{Si=O} + \text{CO}_2 \xrightarrow{25^\circ\text{C}} \equiv\text{Si} \begin{array}{c} \diagup \text{O} \diagdown \\ \diagdown \text{O} \diagup \end{array} \text{C=O}$	1.5	$4.4 \cdot 10^5$

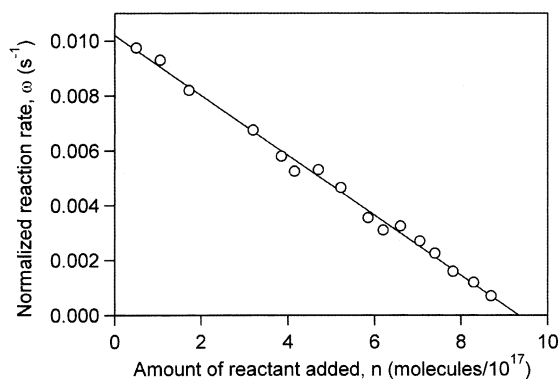


Figure 2. Normalized reaction rate vs the amount of the added monomer for CO addition to $\equiv\text{Si}(-\text{O}-\text{O}-)$ centers (the third reaction in Table 1).

chemisorption step, approximately a third of the initial siloxane centers remained intact at 250 °C.

Effect of the Physical Adsorption on the Observed Kinetics with Surface Radicals. We observed that the kinetics of reactions at the solid–gas interface in our system can be affected by the physical adsorption. In the cases of the interference from such adsorption, only limited kinetic information could be inferred from the volumetric and spectroscopic data. Any quantitatively significant fast adsorption can be formally treated as a fast chemical reaction on the silica surface and will be indistinguishable from the latter on the pressure drop curves, but the ESR spectra then can be taken to determine whether the reaction occurred. We tested several representative monomers from the groups of compounds with weak and strong affinity for the silica surface; such as (1) low boiling point hydrocarbons (ethylene and tetrafluoroethylene) and some simple gases described above (H₂, O₂, CO, and CO₂) and (2) olefins containing polar functionalities (methyl acrylate and allyl alcohol) and high boiling point simple molecules such as SO₂.

No adsorption of ethylene or tetrafluoroethylene has been observed at the ambient temperature (25 °C), when the samples prepared the usual way were converted into nonreactive form by the treatment with H₂. The pres-

Table 2. Reactions of the Surface-Grafted Radicals with Alkenes from the Gaseous Phase

Reaction	Method of activation	N ₀ , volumetric measurements, x10 ⁻¹⁶	N ₀ , Equation 8, x10 ⁻¹⁶	k, L·mol ⁻¹ ·s ⁻¹
$\equiv\text{Si}\cdot + \text{CF}_2\text{CF}_2 \longrightarrow \equiv\text{Si}-\text{CF}_2\text{CF}_2\cdot$	MSi	0.8	0.7	$1.5 \cdot 10^6$
$\equiv\text{Si}\cdot + \text{CH}_2\text{CH}_2 \longrightarrow \equiv\text{Si}-\text{CH}_2\text{CH}_2\cdot$	MSi	5.3	5.8	$1.3 \cdot 10^6$
$\equiv\text{Si}\cdot + \text{CH}_2\text{CH}_2 \longrightarrow \equiv\text{Si}-\text{CH}_2\text{CH}_2\cdot$	RSi	13.1	10.8	$0.72 \cdot 10^6$
$\equiv\text{Si}\cdot + \text{Cyclopentene} \longrightarrow \equiv\text{Si}-\text{Cyclopentyl}\cdot$	MSi	6.4	6.4	$1.4 \cdot 10^6$
$\equiv\text{Si}\cdot + \text{Cyclopentene} \longrightarrow \equiv\text{Si}-\text{Cyclopentyl}\cdot$	RSi	11.9	6.7	$0.34 \cdot 10^6$
$\equiv\text{Si}-\text{O}\cdot + \text{Cyclopentene} \longrightarrow \equiv\text{Si}-\text{O}-\text{Cyclopentyl}\cdot$	MSi	2.8	3.1	$2.1 \cdot 10^6$
$\equiv\text{Si}-\text{Cyclopentyl}\cdot + \text{Cyclopentene} \longrightarrow \equiv\text{Si}-\text{Cyclopentyl}-\text{Cyclopentyl}\cdot + \text{Cyclopentene}\cdot$	MSi	4.4	4.2	$1.5 \cdot 10^4$
$\equiv\text{Si}-\text{O}-\text{Cyclopentyl}\cdot + \text{Cyclopentene} \longrightarrow \equiv\text{Si}-\text{O}-\text{Cyclopentyl}-\text{Cyclopentyl}\cdot + \text{Cyclopentene}\cdot$	MSi	8.4	9.6	$2.9 \cdot 10^4$

sure drop curves corresponded to a change in the volume from V_1 to $V_1 + V_2$ determined previously with He whose adsorption is negligible. The intensity of the ESR spectra of the alkyl radicals formed was directly proportional to the amount of the olefin consumed in the reaction. The radical species were identified by comparison with the previously published data.¹²

The kinetic data displayed linear dependence (as in Figure 2) when they were plotted in the coordinates of eq 8. The number of the radicals determined from the plot and that found in the course of the sample preparation agreed well (Table 2). In addition, the experimental data for the bimolecular reaction yielded a straight line in the semilogarithmic coordinates of the corresponding integrated form of eq 7 (Figure 3):

$$\ln\left(1 - \frac{P_\infty}{P(t)}\right) = \ln\left(1 - \frac{P_\infty}{P_0}\right) - \frac{kP_\infty}{RT}t \quad (9)$$

where $P(t=0) = P_0$ and $P(t=\infty) = P_\infty$ is the pressure in the system at the beginning of the reaction and after its completion.

On the MSi samples, cyclopentene displayed the same general behavior as the low boiling point hydrocarbons, but the reactions on the surface of RSi showed greater deviations. The spectrum of the cyclopentyl radicals grafted onto RSi surface is shown in Figure 4 ($g = 2.0035$; $a(\text{H}_\alpha) = 20.8$, $a(\text{H}_{\beta 1}) = 37.8$ (one H), $a(\text{H}_{\beta 2}) = 33.5$ G (two H) as compared to the reported values¹² of the cyclopentyl radicals: $a(\text{H}_\alpha) = 21.48$ and $a(\text{H}_\beta) =$

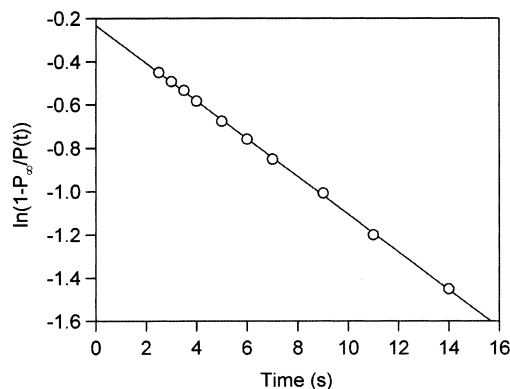


Figure 3. Pressure drop curve in the reaction of tetrafluoroethylene with $\equiv\text{Si}\cdot$ radicals plotted in the coordinates of eq 8.

35.16 G). The probable cause for the dissimilar behavior of the two forms of SiO₂ is the difference in the surface chemistry of the silica and quartz. The former is rich in the silanol groups that may play an important role in the adsorption of the alkene molecules, while the latter is free of the surface hydroxyls, since it is created by the cleavage of the bulk material under vacuum or dry He. The ESR spectra of the cyclopentyl radicals obtained by the reaction with either $\equiv\text{SiO}\cdot$ or $\equiv\text{Si}\cdot$ had intensity directly proportional to the amount of cyclopentene reacted at conversions less than 100% (with respect to the number of the initial radicals in the sample determined in the course of their preparation). However, the reaction retarded notably when additional

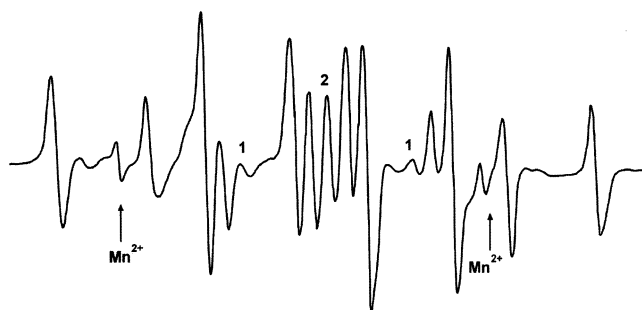


Figure 4. ESR spectrum of the surface-grafted cyclopentyl radicals ($g = 2.0035$; $a(H_\alpha) = 20.8$, $a(H_{\beta 1}) = 37.8$, $a(H_{\beta 2}) = 33.5$ G) formed in the reaction with $\equiv\text{Si}^\bullet$ radical sites. The peaks labeled 1 and 2 are due to the volume trapped radicals $\equiv\text{SiCH}_2^\bullet$ ($g = 2.0030$, $a = 20.1$ G) and $\equiv\text{C}^\bullet$ ($g = 2.0030$), correspondingly. The peaks due to the $\text{Mn}^{2+}/\text{MgO}$ standard are also labeled.

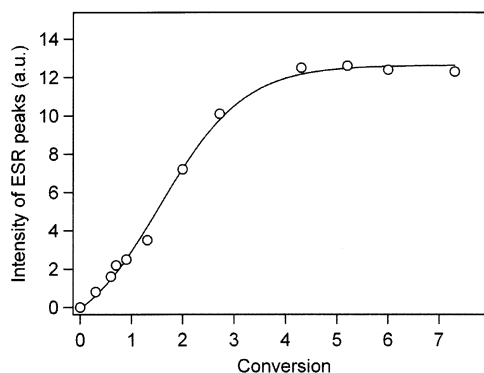


Figure 5. Intensity of the ESR spectrum of allyl radicals vs the depth of conversion of the available surface radicals calculated from the amount of the gaseous reactant (100% conversion = 1).

amounts of cyclopentene were introduced at conversions higher than 100%, whereas the ESR peak intensity steadily decreased. We attribute this reduction in the amount of the surface cyclopentyl radicals to a hydrogen abstraction reaction, which competes successfully with the addition to a double bond. The observed rate constants for allylic hydrogen abstraction in cyclopentene are presented in Table 2. These values are higher by 6 and 3 orders of magnitude than the corresponding rate constants for the hydrogen abstraction from methane ($5.4 \times 10^{-2} \text{ L}\cdot\text{mol}^{-1}\cdot\text{s}^{-1}$) and ethane ($1.6 \times 10^1 \text{ L}\cdot\text{mol}^{-1}\cdot\text{s}^{-1}$) by ethyl radicals on the silica surface.² These differences reflect expected higher stability of the allyl radicals (corresponding differences in the activation energies can be estimated as about 18 and 32 kJ/mol).

The situation is dramatically different for olefins containing polar functional groups. The result for allyl alcohol is shown in Figure 5. The adsorption curves were characteristic for the process of the gas expansion into vacuum, thus showing that the rates were limited by rate of gas flow from V_1 to V_2 . The intensity of the ESR spectra of allyl radicals leveled off at 400–500% conversion with respect to the alkene. No further change was observed when the sample was left at 25 °C for more than 24 h, even after addition of a 50-fold excess olefin, or when the sample was heated for a few hours at 100 °C. Significantly, the number of the allyl radicals was less than 0.1% of the overall number of the initial radicals. The subsequent addition of ethylene to the same sample resulted in the appearance of an intense spectrum of the ethyl radicals, signifying that a large number of the unreacted radical sites remained. We



Figure 6. ESR spectrum of the surface-grafted methyl acrylate radicals ($a(H_\alpha) \approx a(H_\beta) = 19.5$ G) formed in the reaction with $\equiv\text{Si}^\bullet$ radical sites. The peaks labeled with an asterisk are due to the volume trapped $\equiv\text{Si}^\bullet$ radicals ($g_\perp = 2.0003$, $g_\parallel = 2.0018$).

speculate that allyl radicals are formed only upon initial direct collisions with the most accessible surface radicals (e.g., with those on the outermost surface of the MSi grains). The hydroxyl group of the alcohol molecule provides such a strong binding with the silica surface that the diffusion inside the pores of agglomerates is negligible. When an equilibrium pressure of 10^{-1} Torr of allyl alcohol was achieved, the ESR spectrum disappeared likely due to the reaction of the allyl hydrogen abstraction as found in the case of cyclopentene.

The methyl acrylate had a greater surface mobility. The reaction between 5-fold excess olefin and $\equiv\text{SiO}^\bullet$ radicals was completed in 2 h at the pressure in the gaseous phase below 10^{-7} Torr. The ESR spectrum of the addition products (Figure 6), an anisotropic quadruplet with the hyperfine structure constants $a(H_\alpha) \approx a(H_\beta) = 19.5$ G, changed to a triplet with $a(H) = 25$ G when the equilibrium pressure of 10^{-1} Torr of methyl acrylate was achieved. The final spectrum likely corresponds to the isomerization product formed via H-abstraction by the propagating radical from the α -carbon of the several monomer unit long chain.^{13,14}

Sulfur dioxide represents an intermediate case, since the pressure drop curves are representative of the fast physical adsorption, while active radicals ($\equiv\text{SiO}^\bullet$, $\equiv\text{Si}^\bullet$) react so fast that the reaction is complete by the time the sample is placed into the resonator (in ~ 1 min) for recording of the ESR spectrum (an asymmetric singlet with $g = 2.0036$). The fact that the abrupt decrease in the reactant pressure was not caused by the rapid chemical reaction was demonstrated with the inactive silica samples. Samples of MSi and RSi appeared to have centers of specific adsorption of SO_2 , which could be blocked by dosing a large amount of SO_2 (exposure to pressure of 1 Torr) and subsequent pumping down to high vacuum. The additional SO_2 amount could be released only upon temperature increase. Blocking of the active (nonparamagnetic) adsorption centers resulted in the behavior similar to that of hydrocarbons.

These results highlight the limitations of our system in kinetic studies of the radical reactions on the surface of the activated SiO_2 . The chain propagation reactions cannot be studied when (1) hydrogen abstraction reactions or (2) physical adsorption can compete efficiently with the addition to a double bond. The molecules exhibiting low adsorption affinity toward silica (nonpolar hydrocarbons, H_2 , O_2 , CO , and CO_2) are the most suitable for kinetics studies. The chemical reaction rates can be described in a straightforward manner in these well-behaved systems and it is possible to extract values

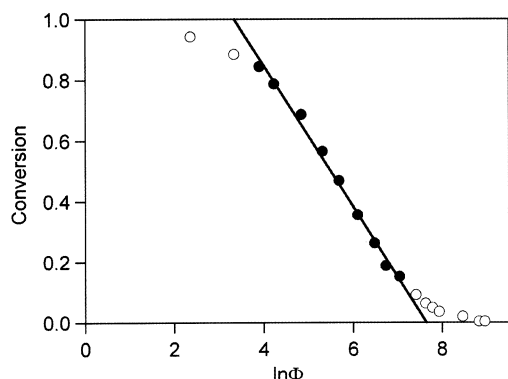


Figure 7. Reaction conversion vs the logarithm of the exposure (in Torr·s) for the addition of SO₂ to ethyl radicals on the surface of RSi (closed circles designate points used in the determination of the rate constants).

of rate constants as high as $10^6 \text{ L}\cdot\text{mol}^{-1}\cdot\text{s}^{-1}$ from volumetric and/or spectroscopic data. For compounds containing functional groups that can strongly bind to the surface of SiO₂ (alcohols), the diffusion to reactive sites may constitute a significant barrier to the progress of the chemical reaction at the interface. In some cases (methyl acrylate, SO₂), the final result is a stoichiometric formation of the surface radical species, which can be used in further transformations with the molecules of the first group. The kinetics of the cross interaction can then be measured. An example of such a cross-interaction is the reactions in the sulfur dioxide-alkene system.

Reaction of Sulfur Dioxide with Alkyl Radicals.

Ethyl Radicals. The ethyl radicals were the least reactive in the addition of SO₂ among the three alkyl radicals investigated (ethyl, tetrafluoroethyl, and cyclopentyl). Thus, the low reactivity permitted the use of high SO₂ pressures and follow the progress of the reaction with the ESR spectroscopy. The kinetics of the interaction of SO₂ with $\equiv\text{SiCH}_2\text{CH}_2\cdot$ on the surfaces of MSi and RSi were studied at a constant SO₂ pressure of approximately 1 Torr. The spectrum of the ethyl radicals was gradually decreasing in intensity, while there appeared and grew a singlet at $g = 2.0047$ corresponding to ethylsulfonyl radicals $\equiv\text{SiCH}_2\text{CH}_2\text{SO}_2\cdot$ (the reported¹⁵ g value in solution is 2.0049, the reported hyperfine splitting of $a(\text{H}_\alpha) = 0.95 \text{ G}$ and $a(\text{H}_\beta) = 1.9 \text{ G}$ was masked by the line width). We found that the rate constant of this pseudo-first-order reaction (constant SO₂ pressure) decreased as the reaction progressed. This can be attributed to the energetic unequivalence of the reactive centers, which has been observed for some slow reactions in these systems.² For a very narrow activation energy distribution ΔE_a , the width of such distribution can be determined from the plots of the depth of conversion θ vs the logarithm of exposure $\Phi(t) = \int_0^t P(\tau) d\tau$ in the intervals $0.2 < \theta < 0.8$ where the plots are almost linear (Figure 7). By extrapolation to $\theta = 0$ (or $\theta = 1$), one finds² (see Supporting Information) the maximum (or minimum) rate constant as $k_{\max} = 1.774/\Phi_{\theta=0}$ (or $k_{\min} = 1/(1.774\Phi_{\theta=1})$). The calculations of the average rate constants, $k_{0.5} = k(\theta=0.5) \approx (k_{\min}k_{\max})^{1/2}$, and the width of distribution, ΔE_a , resulted in $k_{0.5} = 59$ and $93 \text{ L}\cdot\text{mol}^{-1}\cdot\text{s}^{-1}$ for MSi and RSi, correspondingly, and 9.3 and $13.2 \text{ kJ}\cdot\text{mol}^{-1}$ in terms of ΔE_a .

The ethylsulfonyl radicals were stable at 25 °C under ultrahigh vacuum ($\leq 10^{-8}$ Torr) for several days. The ceiling temperature for the formation of the polyethyl-

enesulfone is the highest among alkenes ($> 135^\circ\text{C}$).¹⁵ We can estimate, however, that, according to the Clausius-Clapeyron equation, a reduction in pressure from 760 to 1 Torr will lead to a shift in the ceiling temperature to $> 48^\circ\text{C}$. Therefore, at SO₂ pressures around 1 Torr it may be possible to directly observe the formation and decomposition of the sulfonyl radicals. Indeed, the desorption of SO₂ started when the temperature was raised above 60 °C and the spectrum of the ethyl radicals was restored. The gaseous products in the reaction of the ethylsulfonyl radicals decomposition were reacted with a sample of the freshly prepared $\equiv\text{Si}\cdot$ radicals. The ESR spectrum of the radicals formed was identical to that obtained in a reaction of SO₂ with $\equiv\text{Si}\cdot$ radicals ($g = 2.0036$). We attribute both of them to $\equiv\text{Si}-\text{O}-\text{S}=\text{O}$ radicals. Thus, we directly observed that the reaction of the ethyl radicals with SO₂ is reversible.

At 80 °C, the equilibrium was establishing fast. By changing SO₂ pressure and measuring the spectral intensity, I , of the ethyl radicals (with the initial intensity I_0), we determined the equilibrium constant $K_{\text{eq}} = 3.8 \times 10^5 \text{ L}\cdot\text{mol}^{-1}$ from the experimentally observed dependence of the intensity of the ethyl radicals spectrum on the pressure of the sulfur dioxide in the gas phase:

$$K_{\text{eq}} = \frac{(1 - N/N_0) RT}{N/N_0 P_{\text{SO}_2}} = \frac{(1 - I/I_0) RT}{I/I_0 P_{\text{SO}_2}} \quad (10)$$

The rate constants for the decomposition of the sulfonyl radicals, k_{-1} , determined from the rate of decrease in the sulfonyl radicals intensity or increase in the ESR line intensity of the ethyl radicals were very similar: 4×10^{-5} and $3 \times 10^{-5} \text{ s}^{-1}$, correspondingly. The rate constant for the SO₂ addition at this temperature is then $k_1 = K_{\text{eq}}k_{-1} \sim 15 \text{ L}\cdot\text{mol}^{-1}\cdot\text{s}^{-1}$. This value is within a factor of 4 of the values of $k_{0.5}$ determined at 25 °C, which is comparable to the accuracy of our method and within the distribution width of the rate constants at 25 °C. Thus, an activation energy of the SO₂ addition to ethyl radicals appears to be close to zero. The activation energy of the depropagation reaction was determined by measuring the rates of the reverse reaction from the rate of accumulation of ethyl radicals at two different temperatures. From the rate constants of $5 \times 10^{-4} \text{ s}^{-1}$ and $3 \times 10^{-5} \text{ s}^{-1}$ corresponding to 60 and 80 °C, the activation energy is estimated at $87.6 \text{ kJ}\cdot\text{mol}^{-1}$, which is very close to the value of $83.2 \text{ kJ}\cdot\text{mol}^{-1}$ found in the study of the gas-phase kinetics for this reaction.^{16,17} With the value of the activation energy we can find the rate constant of the dissociation of the sulfonyl radicals at 25 °C. The extrapolation yields $k_{-1} = 1.2 \times 10^{-7} \text{ s}^{-1}$ and, if we use $k_{0.5}$ value for the forward reaction rate constant, equilibrium constant at this temperature is $K_{\text{eq}} = k_1/k_{-1} = 4.9 \times 10^8 \text{ L}\cdot\text{mol}^{-1}$ (or $(0.53-110) \times 10^8 \text{ L}\cdot\text{mol}^{-1}$ for the whole k range). These values are consistent with the observation of the extreme stability of the ethylsulfonyl radicals at 25 °C.

The value of the reaction enthalpy ΔH° can be estimated from the van't Hoff's equation ($d(\ln K)/dT = \Delta H^\circ/RT^2$) and is in the range -78.7 to $-163.6 \text{ kJ}\cdot\text{mol}^{-1}$ corresponding to the distribution of the activation energies of the surface radicals. The lower value seems more reasonable given the activation energy of $87.6 \text{ kJ}\cdot\text{mol}^{-1}$ for the decomposition reaction. A previous experimental study¹⁶ reported $-70.2 \text{ kJ}\cdot\text{mol}^{-1}$ in the gas

phase and MO calculations¹⁸ found $-82.8 \text{ kJ}\cdot\text{mol}^{-1}$. The rate constants for the slower ethyl radicals (6.4 and $9.0 \text{ L}\cdot\text{mol}^{-1}\cdot\text{s}^{-1}$ for MSi and RSi, respectively) are then more representative of the true reactivity of the ethyl radicals toward SO_2 . The higher reactivity may then be a consequence of the increased surface coverage at high SO_2 pressure and a higher local acting SO_2 concentration in the vicinity of the surface. Indeed, the activation energy for SO_2 addition is then $10.0 \text{ kJ}\cdot\text{mol}^{-1}$ ($k_1 = 6.4$ and $15 \text{ L}\cdot\text{mol}^{-1}\cdot\text{s}^{-1}$ at 25 and 80°C , respectively) in close agreement with the reaction enthalpy and activation energy of the reverse reaction ($87.6 - 78.7 = 8.9 \text{ kJ}\cdot\text{mol}^{-1}$). This value is also in agreement with the data in the gas phase ($13.0 \text{ kJ}\cdot\text{mol}^{-1}$) and MO calculations ($11.3 \text{ kJ}\cdot\text{mol}^{-1}$) for this reaction.

The reaction enthalpy for addition of SO_2 implies that C–S bond formed in sulfonyl radicals is much weaker than a typical C–S bond ($\sim 272 \text{ kJ}\cdot\text{mol}^{-1}$). In solution, the formation of the polysulfones typically results in $\sim -84 \text{ kJ}\cdot\text{mol}^{-1}$ per monomer.¹⁵ Thus, using typical bond energies one can estimate that when the second C–S bond is formed with an electron-deficient center at a remote C atom, this C–S is much stronger having a more typical value of $271 \text{ kJ}\cdot\text{mol}^{-1}$ (from $-\Delta H^\circ = E_{\text{C-C}} + E^{(1)}_{\text{C-S}} + E^{(2)}_{\text{C-S}} - E_{\text{C=C}}$). We can, therefore, assign a destabilization energy of $\sim 192 \text{ kJ}\cdot\text{mol}^{-1}$ to the electrophilic character of the sulfonyl radicals.

Cyclopentyl Radicals. The equilibrium of the formation and decomposition of the cyclopentylsulfonyl radicals was very labile. The initial spectrum of the cyclopentyl radicals transformed to an anisotropic singlet ($g = 2.0045$) upon the treatment with an equimolar amount of SO_2 . However, the initial spectrum was easily restored under evacuation even at 25°C (reported¹⁵ ceiling temperature for the polycyclopentenesulfone is 103 vs $>135^\circ\text{C}$ for the polyethylene-sulfone). The rate constant of the monomolecular decomposition reaction was found to be $2.5 \times 10^{-4} \text{ s}^{-1}$ from the ESR data in accordance with the equation

$$\ln\left(1 - \frac{I}{I_\infty}\right) = -kt \quad (11)$$

where I_∞ is the intensity of the cyclopentyl radicals at the completion of the decomposition.

As mentioned in the section on the physisorption, the exposure of the MSi to 1 Torr pressure of SO_2 blocked the most active centers of the SO_2 adsorption, so that its physisorption in the subsequent experiments on the same sample can be neglected. Since the original radical species were easily restored upon removal of the SO_2 , thermodynamic and kinetic parameters in this system could be derived by two different means.

The equilibrium constant at 25°C $K_{\text{eq}} = 6.8 \times 10^7 \text{ L}\cdot\text{mol}^{-1}$ determined from the ESR data and an equilibrium pressure of SO_2 (eq 10) was in a very good agreement with the value $K_{\text{eq}} = 8.7 \times 10^7 \text{ L}\cdot\text{mol}^{-1}$ based on the ESR and volumetric (chemisorption) data (eq 12, where $N_{\text{SO}_2}^{\text{ads}}$ is the amount of SO_2 chemisorbed, N and N_0 are the current and initial number of the alkyl radicals):

$$K_{\text{eq}} = \frac{N_{\text{SO}_2}^{\text{ads}}}{N} \frac{RT}{p_{\text{SO}_2}} = \frac{N_{\text{SO}_2}^{\text{ads}}}{N_0} \frac{RT}{I_0 p_{\text{SO}_2}} \quad (12)$$

A finite low SO_2 pressure was easily obtained after cycling a sample through 1 Torr of SO_2 pressure. The

initial rate of the sulfonyl radical formation determined under approximately constant SO_2 pressure obeys a pseudo-first-order rate equation, because the reverse reaction can be neglected. The rate constant found from the decreasing intensity of the cyclopentyl radicals at very low conversions ($<10\%$) resulted in the value of $k_1 = 1.7 \times 10^4 \text{ L}\cdot\text{mol}^{-1}\cdot\text{s}^{-1}$. Alternatively, the equilibrium constant can be used to evaluate the rate constant of the bimolecular SO_2 –cyclopentyl addition as $k_1 = k_{-1}K_{\text{eq}} = (1.7\text{--}2.2) \times 10^4 \text{ L}\cdot\text{mol}^{-1}\cdot\text{s}^{-1}$ in a good agreement with the direct measurement. The bond between sulfur of SO_2 and secondary carbon of an allyl monomer is much more labile than the corresponding bond of the primary alkyl radicals in terms of both the rate of formation and decomposition. The method of the “stopped chain growth” applied in this work is unique in allowing a direct experimental observation of the reversibility of a radical addition reaction. No postulated mechanism is needed to establish such a reversibility, and the reaction can be cycled back and forth by simply changing the pressure of the reagent in the gas phase.

Our kinetic data on the reactivity of alkyl radicals with SO_2 also points out to the difference between the reactions of the formation of the sulfonyl radicals at the solid surface and in the gaseous or liquid phases, the homogeneous kinetics being several orders of magnitude faster. The rate constant of the SO_2 addition to cyclopentyl radicals in chlorocyclopentene was found to be $\sim 8 \times 10^9 \text{ L}\cdot\text{mol}^{-1}\cdot\text{s}^{-1}$.¹⁹ Moreover, the addition reaction of ethyl radicals to SO_2 in the gaseous phase was also found to proceed with a similarly high rate: values of 5.5×10^5 and $1.8 \times 10^8 \text{ L}\cdot\text{mol}^{-1}\cdot\text{s}^{-1}$ were reported.^{16,17} The latter value is probably more accurate, because of the aerosol formation problem¹⁷ with the technique used in the first study.¹⁶ At present, the source for such a large discrepancy between the reactivity of the surface and volume radicals is unclear. However, the activation energy and thermodynamic parameters for the SO_2 addition to radical sites on silica seem to be in agreement with other data.

Tetrafluoroethyl Radicals. The tetrafluoroethyl radicals were the most reactive toward SO_2 (the reaction occurred at SO_2 pressure $\leq 10^{-6}$ Torr). However, we did not observe the reversibility of the SO_2 addition in this case. A similar reaction with the hexafluoropropyl radicals was slower, but also irreversible. The sulfonyl radicals remained intact even at the elevated temperatures up to 100°C . By comparing this observation with the results for the ethylsulfonyl radicals, we can put the upper limit on the decomposition rate constant at $k_{-1} < 10^{-9} \text{ s}^{-1}$. The irreversibility coupled with the high rate deprived us from the means utilized earlier to derive the kinetics parameters for this system. However, despite the deficiency of the experimental method the lower limit of the addition rate constant can be estimated from the time dependence of the intensity of the spectrum of the tetrafluoroethyl radicals. When a 5-fold excess of SO_2 was added to a sample of the tetrafluoroethyl radicals, the fast adsorption process took place reducing the equilibrium pressure to $\leq 10^{-6}$ Torr. However, the slow disappearance of the tetrafluoroethyl radicals obeyed the second-order kinetics in a closed volume:

$$\frac{dN_{\text{R}}}{dt} = -kN_{\text{R}} \frac{N_{\text{SO}_2}^0 - (N_{\text{R}}^0 - N_{\text{R}})}{V}$$

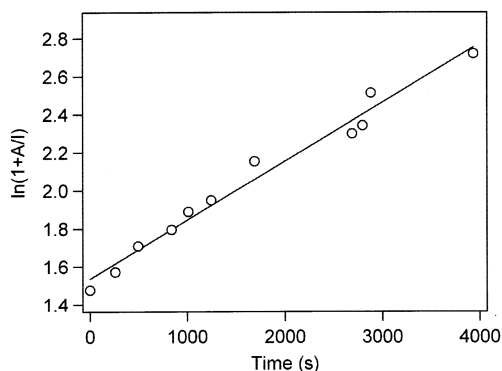


Figure 8. Kinetics data for the second-order reaction of the SO₂ addition to tetrafluoroethyl radicals in a closed volume.

where V is the active volume and N designates the number of species (SO₂ molecules or radicals R) and the superscript 0 represents the initial quantity. The integrated form of this equation:

$$\ln \frac{N_R}{N_{SO_2} - (N_R^0 - N_R)} \frac{N_{SO_2}^0}{N_R^0} = -\frac{k}{V}(N_{SO_2}^0 - N_R^0)t$$

can be conveniently rewritten as

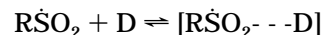
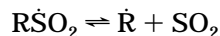
$$\ln\left(1 + \frac{A}{I}\right) = \ln\left(1 + \frac{A}{I_0}\right) + \frac{k}{V} \frac{N_R^0}{I_0} At \quad (13)$$

by defining a constant $A = I_0(N_{SO_2}^0/N_R^0 - 1)$, which contains only the initial parameters for the system. We observed a linear dependence of $\ln(1 + A/I)$ vs time as expected from eq 13 (Figure 8). A problem with the rate constant found in this manner, $1.2 \times 10^5 \text{ m}^2 \cdot \text{mol}^{-1} \cdot \text{s}^{-1}$ (a product of $k/V = 6 \times 10^3 \text{ mol}^{-1} \cdot \text{s}^{-1}$ in eq 13 above and the sample surface area of $\sim 20 \text{ m}^2$), is that its respective three-dimensional value has to be determined based on the concentration of SO₂ either in a gaseous phase or within a thin surface adsorption layer (presumed to be several angstroms thick). The two approaches lead to two drastically different values for the rate constant of the SO₂ addition to the tetrafluoroethyl radicals: $> 10^7 \text{ L} \cdot \text{mol}^{-1} \cdot \text{s}^{-1}$ and $\sim 2 \times 10^{-5} \text{ L} \cdot \text{mol}^{-1} \cdot \text{s}^{-1}$. The latter number seems unreasonable, because the reaction (with SO₂ pressure $\leq 10^{-6}$ Torr) proceeds much faster than an analogous process for the ethyl radicals (with SO₂ pressure of 1 Torr), for which the rate constant of the SO₂ addition is already low, $(6-9) \times 10^1 \text{ L} \cdot \text{mol}^{-1} \cdot \text{s}^{-1}$. Therefore, we favor a model that takes a gaseous concentration of SO₂ as its acting concentration, and, respectively, the reaction of sulfur dioxide with $\equiv\text{SiCF}_2\text{CF}_2\cdot$ radicals occurs at the rates exceeding $10^7 \text{ L} \cdot \text{mol}^{-1} \cdot \text{s}^{-1}$. We can conclude that a perfluoroalkyl radical makes a much more stable sulfonyl radical (higher $K_{eq} > 10^7/10^{-9} = 10^{16} \text{ L} \cdot \text{mol}^{-1}$) and is much more reactive (higher k_i) in the SO₂ addition than nonfluorinated radicals (i.e., tetrafluoroethyl > cyclopentyl > ethyl).

Reactivity of Sulfonyl Radicals in Addition of Alkenes. Surprisingly, all of the sulfonyl radicals generated turned out to be completely inactive in the subsequent addition reactions with olefin monomers. All attempts with variations in the olefin concentrations (with pressures up to 1 atm) and in temperature (up to 100 °C) were unsuccessful. Given that we can detect a fraction of radicals as small as 0.01%, the upper limit

of the equilibrium constant can be estimate as $\sim 10^{-6} \text{ L} \cdot \text{mol}^{-1}$. The failure to observe this reaction may signify a thermodynamic instability of $R\text{-SO}_2\text{-}R\cdot$ radicals: the enthalpy of reaction is close to zero (as estimated from the typical bond energies), while the entropic change is negative and, therefore, the entropic factor is strongly unfavorable, especially at the low pressures. Semi-empirical MO calculations also show that not only the absolute value of ΔH° for the C₂H₄ addition to sulfonyl radicals is reduced by $+48.3 \text{ kJ} \cdot \text{mol}^{-1}$ to $-34.7 \text{ kJ} \cdot \text{mol}^{-1}$ with respect to the addition of SO₂ to ethyl radicals, but also the activation energy grows from 11.3 to 27.7 kJ·mol⁻¹.¹⁸ However, the analysis above of our activation energy data and thermochemical data on polysulfones led to a much smaller estimate for $\Delta H^\circ \sim -5 \text{ kJ} \cdot \text{mol}^{-1}$ for the C₂H₄ addition. The activation energy can then correspondingly be larger by the same amount, i.e., $E_a \sim 58 \text{ kJ} \cdot \text{mol}^{-1}$. Given that the entropy change for this reaction is primarily due to the removal of a gas-phase reactant (e.g., ethylene), we can evaluate²⁰ the equilibrium constant using $\Delta H^\circ \sim -5 \text{ kJ} \cdot \text{mol}^{-1}$ and $\Delta S^\circ \approx S^\circ(\text{C}_2\text{H}_4) = 219.3 \text{ J} \cdot \text{mol}^{-1} \text{ K}^{-1}$ to be $K_{eq} = 1.8 \times 10^{-8} \text{ L} \cdot \text{mol}^{-1}$, consistent with our inability to observe this addition reaction.

Our observations contrast with the data in liquid solutions, where sulfonyl radicals do react with a double bond to form sulfones.²¹ It has been argued that in solution environment the reaction takes a pathway, which involves some complex formation between reagents or a donor monomer and sulfonyl radicals.¹⁹ Our data seem to be in line with the suggested mechanism: not only the reactivities of the alkyl radicals toward SO₂ and sulfonyl radicals toward alkenes are dramatically different (which is consistent with the mechanism of a consecutive addition of the monomers in the alternating copolymerization), but also the $R\text{-SO}_2\text{-}R\cdot$ radicals do not appear to be stable under normal conditions. Therefore, if the formation of the complex between $R\text{-SO}_2\cdot$ radicals and a donor monomer D is possible, the addition reaction will not proceed until another SO₂ molecule arrives at the [(growing chain-SO₂ radical)- D monomer] complex:



Conclusions

Chemically and mechanically activated silica was used to provide a well-defined system, with which to study kinetics of the cross-reactions of the radical copolymerization in the regime of the "stopped chain growth". The system provided an effective combination of the volumetric techniques and ESR spectroscopy for the determination of the rate constants and identification of the reactive species. The setup was used to characterize the reactions of the native para- and diamagnetic defects on the surface of the activated silica with the simple molecules from the gas phase (H₂, O₂, CO, CO₂, SO₂, and simple substituted alkenes). The rate constants up to $10^6 \text{ L} \cdot \text{mol}^{-1} \cdot \text{s}^{-1}$ could be determined with the present method.

The ability to exchange monomers after each addition step was used to probe the reaction mechanism and kinetics of alternating copolymerization of sulfur dioxide with olefins. There were limitations imposed by the

adsorption of polar monomers, which were overcome in the case of the SO₂ addition reactions by determining the rates of the reverse reactions and the equilibrium constants or by blocking the high affinity centers of physisorption by the exposure to a high SO₂ pressure followed by evacuation. The reversibility of the SO₂ addition to alkyl radicals was observed in *real time* with equilibrium constants decreasing in the order $K(\text{SiC}_2\text{F}_4) > K(\text{SiC}_2\text{H}_4) > K(\text{SiC}_5\text{H}_{10})$. The S–C bond in polysulfones, therefore, appears to be more labile for the substituted monomers with higher electron donating properties. The drastically different reactivities of SO₂ with alkyl radicals and of alkenes with sulfonyl radicals seem consistent with the view that the alternating radical copolymerization in the liquid phase proceeds via a “complexation” mechanism, that is “sulfonyl radical–alkene complexes” are the effective monomers for the propagating chain, while alkenes by themselves are totally unreactive toward sulfonyl radicals under the normal conditions. The observed discrepancy between the rate constants of the SO₂ addition reactions on the surface of silica and the same reactions in the gas or liquid phase requires further investigation, although activation energies and reaction enthalpies appear to be consistent with the previous experiments and MO calculations.

Supporting Information Available: Figure showing the extent of the reaction, a table giving data for the characterization of the surface species formed under various treatments during the thermal activation of the methoxylated silica, and text giving the derivation of the expressions for the rate constants in the case of a nonuniform activation energy

distribution of the reactive centers. This material is available free of charge via the Internet at <http://pubs.acs.org>.

References and Notes

- (1) Bobyshev, A. A.; Radtsig, V. A. *Kinet. Catal.* **1991**, *31*, 810.
- (2) Bobyshev, A. A.; Radtsig, V. A.; Senchenya, I. N. *Kinet. Catal.* **1991**, *31*, 815.
- (3) Bobyshev, A. A.; Kazanskii, V. B.; Kibardina, I. R.; Shelimov, B. N. *Kinet. Catal.* **1992**, *33*, 293.
- (4) Korolkova, E. M.; Radtsig, V. A.; Melnikov, M. Y. *Dokl. Akad. Nauk* **1993**, *331*, 188.
- (5) Roginskaya, M. V.; Razskazovskii, Yu. V.; Melnikov, M. Ya. *Kinet. Catal.* **1992**, *33*, 521.
- (6) Wovchko, E. A.; Camp, J. C.; Glass, J. A.; Yates, J. T., Jr. *Langmuir* **1995**, *11*, 2592.
- (7) Brei, V. V.; Gunko, V. M.; Khavryuchenko, V. D.; Chuiko, A. A. *Kinet. Catal.* **1991**, *31*, 1019.
- (8) Kabanov, V. A.; Zubov, V. P.; Semchikov, Yu. D. *Complex-Radical Polymerization* (in Russian); Khimiya: Moscow, 1987.
- (9) Golubev, V. B.; Bulgakova, L. M.; Lunina, A. V.; Gromov, D. G.; Vezenov, D. V. *Polym. Sci. USSR* **1991**, *33*, 1047.
- (10) Morterra, C.; Low, M. J. D. *J. Phys. Chem.* **1969**, *73*, 321.
- (11) Morterra, C.; Low, M. J. D. *J. Phys. Chem.* **1969**, *73*, 327.
- (12) Radtsig, V. A. *Kinet. Catal.* **1983**, *24*, 173.
- (13) Sugiyama, Y. *Bull. Chem. Soc. Jpn.* **1997**, *70*, 1827.
- (14) Best, E. M.; Kasai, P. H. *Macromolecules* **1989**, *22*, 2622.
- (15) Gilbert, B. C.; Norman, R. O. C.; Sealy, R. C. *J. Chem. Soc., Perkin Trans. 2* **1975**, 308.
- (16) Good, A.; Thynne, J. C. J. *Trans. Faraday Soc.* **1967**, *63*, 2720.
- (17) James, F. C.; Kerr, J. A.; Simons, J. P. *J. Chem. Soc., Faraday Trans. 1973*, *2*, 2124.
- (18) Gozdz, A. S. *Macromolecules* **1990**, *23*, 910.
- (19) Golubev, V. B. *Polym. Sci.* **1994**, *2*, 244.
- (20) NIST-JANAF Thermochemical Tables, <http://webbook.nist.gov>.
- (21) Ivin, K. J.; Rose, J. B. *Adv. Macromol. Chem.* **1968**, *1*, 336.

MA021122+